PERFORMANCE COMPARISON OF ACTIVE AND SEMI-ACTIVE REGULATORS SMC & LQR IN A QUARTER-CAR MODEL

URSZULA FERDEK
JAN ŁUCZKO
Cracow University of Technology, Faculty of Mechanical Engineering, Krakow, Poland
e-mail: uferdek@mech.pk.edu.pl; jluczko@mech.pk.edu.pl

A b s t r a c t

In this paper an analysis is performed on a quarter-car model of car suspension, with semi-active and active damper, utilizing sliding mode (SMC) and linear-quadratic control (LQR). The effect of control parameters and time delays in the transmission of control signal on the factors related to the safety and comfort of driving is investigated. The results obtained from numerical simulations are shown in the form of frequency characteristics for several selected performance factors.

Keywords: active damping, semi-active damping, vibration reduction, car suspension

1. Introduction

For the purpose of checking the chosen concepts of active or semi-active control of car suspension, either quarter-car [1-6,9,13,17,20,21] or less often half-car [14-16] vehicle models are used. These usually are linear models with two- or four-degrees of freedom depending on the chosen type. They consist of both spring-supported masses (¼ or ½ car body) and non-spring supported ones (wheels with the reduced mass of the suspension system). The performance factor of the acting vibroisolation system, should provide a compromise between the passengers' comfort level and their safety during the drive [1,3,8,9]. Several indexes of the driving comfort are introduced, either related to the displacements and velocities [2,5,14,17,21] or to the accelerations [3,4] of the so-called spring-supported mass, i.e. car body. Most often the values used for this purpose are either mean or peak ones. The measure of safety level is on the other hand derived form the net reaction or its dynamic component [1, 3], e.g. Eusam's index. With the decrease of net reaction, the adhesion of the wheels and the steering decreases as well. The same happens to the performance of force transmission of the drive and braking.

In the numerical simulations performed to analyze the behavior of the driving vehicle, the knowledge of the function describing the kinematic excitation acting

on the vehicle, is essential. Several different approaches to describing the irregularities in the road are presented in literature. The road profile can be defined using a random function [17] or a harmonic one of constant [1,2,9,21] or modulated frequency. If the vehicle is crossing some obstacles (e.g. bumps) either impulse function of unit step type [1] or other of more complex form [2,6,8] are used.

In the active systems, several different types of control can are used. These are usually based on the algorithms for the linear-quadratic regulation (LQR) [4,12], PID regulation [10,14,20] or sliding mode control (SMC) [2,5,6,14,15,17,18,21]. Theoretically in the case of active damping, there are no limitations imposed on the function defining the control force.

In the semi-active systems [1,3,4,7,8,19] the basic restriction imposed on the control, is based on the condition of preventing the introduction of energy to the system. This condition is fulfilled if the product of control force and the velocity of spring-supported mass to the non-spring supported one (power) is less then zero. It is most often considered for the purpose of controlling the damping properties of magneto-rheological dampers [11,16].

In this study, an emphasis was placed on analyzing the efficiency of two active control algorithms, utilizing LQR and SMC regulation, respectively. Additionally an analysis of performance of semi-active systems, based on these regulators, was made. In the numerical simulations, the influence of time delay present between the control signal and the actuator was included.

2. Quarter-car suspension model

In this study a quarter-car model was used as seen in Figure 1. The motion of both masses: the non-spring-supported m_w and the spring-supported one m_b are defined by variables y_w and y_b, displacement $w(t)$ is the given kinematic excitation, while $u(t)$ is the active or semi-active system influence on the mass elements m_w and m_b. Parameters k_w and c_w define the spring and damping properties of the wheel, while the parameters k_b and c_b define the properties of the suspension system. Due to the negligible effect of the damping of the rubber on the results, this parameter is omitted in the analysis (c_w=0).

The motion of the system around the static equilibrium position can be written using the following matrix differential equation:

$$\mathbf{M}\ddot{\mathbf{y}} + \mathbf{C}\dot{\mathbf{y}} + \mathbf{K}\mathbf{y} = \tilde{\mathbf{B}}u + \tilde{\mathbf{F}}w(t) \tag{1}$$

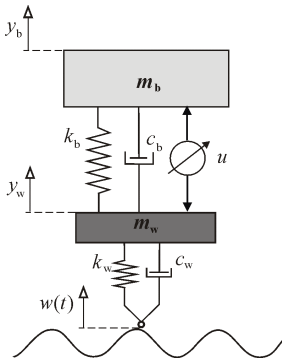

Fig. 1. Quarter-car model

where $\mathbf{y}=[y_w, y_b]^T$. Matrices: mass $\mathbf{M}$, damping $\mathbf{C}$ and stiffness $\mathbf{K}$ are given as:

$$\mathbf{M}=\begin{bmatrix} m_w & 0 \\ 0 & m_b \end{bmatrix} \qquad \mathbf{C}=\begin{bmatrix} c_b & -c_b \\ -c_b & c_b \end{bmatrix} \qquad \mathbf{K}=\begin{bmatrix} k_w+k_b & -k_b \\ -k_b & k_b \end{bmatrix} \tag{2}$$

while the $\tilde{\mathbf{B}}$ and $\tilde{\mathbf{F}}$ vector are of a form:

$$\tilde{\mathbf{B}}=\begin{bmatrix} -1 \\ 1 \end{bmatrix} \qquad \tilde{\mathbf{F}}=\begin{bmatrix} k_w \\ 0 \end{bmatrix} \tag{3}$$

A modified state space vector is introduced, one that includes generalized velocities:

$$\mathbf{x}=\begin{bmatrix} \mathbf{x}_1 \\ \mathbf{x}_2 \end{bmatrix}=\begin{bmatrix} \mathbf{y} \\ \dot{\mathbf{y}} \end{bmatrix} \tag{4}$$

thus allowing to write Eq. (1) in the form of first-order differential equation:

$$\dot{\mathbf{x}}=\mathbf{A}\mathbf{x}+\mathbf{B}u+\mathbf{F}w \tag{5}$$

There's a relation between matrix $\mathbf{A}$ and matrices present in Eq. (1):

$$\mathbf{A}=\begin{bmatrix} \mathbf{0}^{(2\times2)} & \mathbf{I}^{(2\times2)} \\ -\mathbf{M}^{-1}\mathbf{K} & -\mathbf{M}^{-1}\mathbf{C} \end{bmatrix} \tag{6}$$

in which matrices $\mathbf{0}^{(2\times2)}$ and $\mathbf{I}^{(2\times2)}$ are respectively the empty and singular matrix of size 2×2. The same relation is for the matrices:

$$\mathbf{B}=\begin{bmatrix} \mathbf{0}^{(2\times1)} \\ \mathbf{M}^{-1}\tilde{\mathbf{B}} \end{bmatrix} \qquad \mathbf{F}=\begin{bmatrix} \mathbf{0}^{(2\times1)} \\ \mathbf{M}^{-1}\tilde{\mathbf{F}} \end{bmatrix} \tag{7}$$

where $\mathbf{0}^{(2\times1)}$ is an empty vector of length 2.

3. Linear-quadratic regulator (LQR)

Linear-quadratic regulation is often used for the vibration reduction [4,12]. The control signal generated by the controller, depends on the actual state of the system:

$$u = -\mathbf{L}\mathbf{x} \tag{8}$$

The control if found using the minimal performance factor condition:

$$J = \int_0^\infty \left[\mathbf{x}^T \mathbf{Q}\,\mathbf{x} + Ru^2\right] dt \tag{9}$$

in which **Q** is a positive half-defined weight matrix related to the state vector, while R in case of a single-input control is a positive weight coefficient When minimizing the car body vibration, it can be assumed that: $\mathbf{Q}$=diag(0, q_x, 0, q_v). Such a form of the weight matrix should ensure the minimum of the second and fourth of state vector variables i.e. the displacement and velocity of the spring-supported mass. After the matrix **W**, which is the solution to the Ricatti equation:

$$\mathbf{A}^\mathbf{T}\mathbf{W} + \mathbf{W}\mathbf{A} - \mathbf{W}\mathbf{B}R^{-1}\mathbf{B}^T\mathbf{W} + \mathbf{Q} = \mathbf{0} \tag{10}$$

is obtained, matrix **L** (transposed vector) can be found from formula:

$$\mathbf{L} = R^{-1}\mathbf{B}^T\mathbf{W} \tag{11}$$

4. Sliding mode control (SMC)

An alternative option for the active control of the car suspension, is to use the algorithm of sliding mode control (SMC) [2,5,6,14,15,17,21]. During the process of regulation, two phases can be distinguished: the approach phase which lasts till the point that describes the dynamics of the system, reaches the so-called "sliding plane", and the sliding phase. In the analyzed example, the sliding plane can be described using formula:

$$S = \kappa_x e + \kappa_v \dot{e} \tag{12}$$

in which e is the regulation error. When minimizing the displacements of the spring-supported mass, this error can be assumed to be equal to the displacement of this mass, meaning $e=x_2=y_b$. Therefore, after the introduction of the transposed vector:

$$\mathbf{D} = [0, \kappa_x, 0, \kappa_v] \tag{13}$$

the sliding plane equation cane be written in the form:

$$S = \mathbf{D}\mathbf{x} \tag{14}$$

The approach to the sliding plane is ensured by the so-called compensation (equivalent) component of the control, which can be found from the relation:

$$\dot{S} = \mathbf{D}\dot{\mathbf{x}} = \mathbf{D}(\mathbf{A}\mathbf{x} + \mathbf{B}u + \mathbf{F}w) = 0 \tag{15}$$

The product **DF** of transposed vector **D** and vector **F** defined this way is equal to zero, which means that the equivalent component in this example does not depend on the excitation. If the model is well-known and no disturbance is present, the equivalent control defined by formula:

$$u^{eq}(t) = -(\mathbf{DB})^{-1}\mathbf{DA}\mathbf{x} \tag{16}$$

compensated all the other forces acting on the spring-supported mass, and in theory the vibration of the system can be completely damped. Most often the parameters of the model are not known, while the structure of the system is more complex, with the model being usually nonlinear. In a physical system, both the disturbances of control signal and the time delay between the regulator and actuator are present. Due to these reasons, additional discontinuous control is added in the form of a switching component: $u^{sw}(t)$ (switching control):

$$u^{sw}(t) = -K^{sw}(\mathbf{DB})^{-1}\,\mathrm{sgn}(S) = -K^{sw}(\mathbf{DB})^{-1}\,\mathrm{sgn}(\mathbf{Dx}) \tag{17}$$

The final form of the control signal is given by formula:

$$u(t) = -(\mathbf{DB})^{-1}[\mathbf{DA}\mathbf{x} + K^{sw}\,\mathrm{sgn}(\mathbf{Dx})] \tag{18}$$

in which K^{sw} is found based on the numerical simulation.

5. Semi-active systems

In the semi-active systems, the realization of actual LQR or SMC control is not possible, because of their active behavior. Therefore, these algorithms are usually modified to ensure that the momentary power is always negative (which means that no energy is introduced to the system). Additionally, some sort of limitation is usually imposed on the control (clipped LQR [12]). For such semi-active control systems the control is found using the equation:

$$u^{clipped} = \varphi(u, u_{\max}, v) \tag{19}$$

in which φ is of form:

$$\varphi(u, u_{\max}, v) = \begin{cases} 0 & vu \geq 0 \\ u & vu < 0 \quad \text{i} \quad |u| < u_{\max} \\ u_{\max} & vu < 0 \quad \text{i} \quad u \geq u_{\max} \\ -u_{\max} & vu < 0 \quad \text{i} \quad u \leq -u_{\max} \end{cases} \tag{20}$$

where u is the control, found from the condition of minimizing the functional (9) or from Eq. (18), $u_{\max}$ is the maximal permissible value of control, while $v=v_b-v_w$ is the velocity of spring-supported mass with relation to the non-spring-supported one. The effectiveness of semi-active damping can be estimated through the numerical simulations.

6. Results of numerical simulations

The proposed algorithms of active and semi-active damping are based on the assumption, that the model of the system is a precise description of the actual physical system. In practice, some sort of uncertainty of the model needs to be taken into account, mostly due to the simplified and usually linear description of the object and inaccurately determined parameters. Additionally, the disturbances and the time delay between the control signal and the actuator, influence the performance of regulation. The analysis below, is limited to finding the sensitivity of the designed regulator to the time delay only, under the assumption that the acting force U is related to the control signal u by the equation of first-order filter:

$$\dot{U} = -\sigma(U - u) \tag{21}$$

where σ is the inverse of time constant.

In the numerical calculations, the following values of parameters of the quarter-car model were chosen: m_w=28kg, m_b=510kg, k_w=180000N/m, k_b=20000N/m, c_b=1000Ns/m.

Below, the effect of the parameters, present in the control algorithms LQR and SMC on the indexes, describing the driving comfort and safety, is presented. In order to measure the discomfort experienced by the passengers, both the displacement and velocity characteristics of the spring-supported mass are used. The driving safety is measured using the Eusam index W_E, which calculates the wheel-surface adhesion. Eusam index is defined as a ratio of the maximal force to the static force acting on the wheel.

The values of indexes related to the driving comfort and safety reach maximum in different regions of excitation frequency. In case of the vibration of frequency within the first vibration mode region, the car body displacements are dominant, which means that the driving comfort is worse. When the frequency of vibration is within the region close to the second natural mode, the displacements of car suspension are larger, and the wheel adhesion to the road is decreased. In order to evaluate the global performance of the regulator, it is advised to use either the frequency characteristics of the system or analyze the response of the system to the excitation of modulated frequency e.g. function „chirp”. Below function of „chirp” type is used with the variable amplitude of the excitation. The proposed modification, is introduced due to the fact, that the frequency of excitation related to the velocity of the vehicle is increased, with the increase in amplitude, or more precisely with the decrease in the irregularities of the road. The noticeable effect of such a correction to the excitation, are more realistic values of Eusam index. Without this modification, when the amplitude of excitation is too high, the Eusam index is negative within the high frequency range (which denoted the loss of adhesion), and practically independent of the used vibroisolation system.

Further, it was assumed, that with the increase of the excitation frequency, the amplitude decreases according the formula:

$$a = \frac{\alpha_1}{(\alpha_2 + \omega)^2} \tag{22}$$

The value of coefficients α_1 and α_2 are found from the condition, that the amplitude value close to the first resonance frequency (ω=8.396 rad/s) is equal α_0=0.005m, and around the second resonance frequency (ω=84.39 rad/s) the amplitude is 0.0004m (α_1=914.2631 ms^2/rd^2 and α_2=21.3806 rd/s). Additionally it is assumed, that the frequency increases proportionally to the square of time:

$$\omega = \omega_1 + \varepsilon t^2 = \omega_1 + (\omega_2 - \omega_1)(t/T_{sim})^2 \tag{23}$$

while in the region, limited by the frequencies ω_1 and ω_2 (ω_1=1 rd/s, ω_2=100 rd/s) both resonance frequencies are present. Parameter T_{sim} is the large enough duration of simulation. Fig. 2 shows the kinematic excitation in the function of time:

$$w(t) = a\sin(\omega_1 t + \varepsilon t^3/3) \tag{24}$$

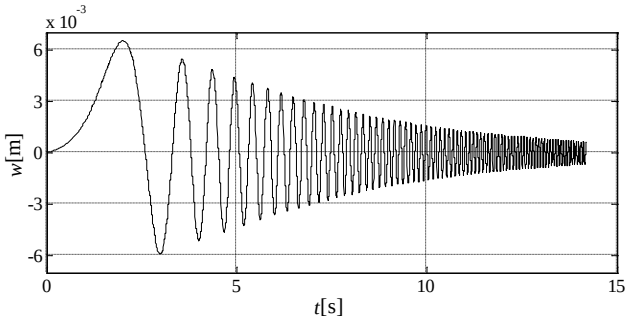

Fig. 2. Kinematic excitation $w(t)$

The effectiveness of both of the considered regulators depends on the three parameters (q_x, q_v and R for LQR, κ_x, κ_v and K^{sw} for SMC). As the units of parameters in both of this cases are different, it is better to use dimensionless control parameters, defined as follows: $\alpha_x=q_xK_x^2$, $\alpha_v=q_vK_v^2$, $\rho=RK_u^2$ for LQR and $\beta_x=\kappa_xK_x$, $\beta_v=\kappa_vK_v$, $\gamma=K^{sw}/\omega_0$ for SMC, with: $K_x=a_0$, $K_v=\omega_0a_0$, $K_u=k_ba_0$, $\omega_0=\sqrt{k_b/m_b}$.

In case of a linear-quadratic regulator, one of the parameters: α_x, α_v or ρ, can be chosen arbitrarily, due to the form of functional (9). In the numerical simulation presented here, the value α_v=1 was chosen. The ratio between the parameters α_x and ρ highly influences the results. With the increase of this ratio the amplitudes of displacements, velocities and accelerations are decreased, especially within the range of the first resonance. Additionally, the Eusam index is decreased, which means that the wheel adhesion to the road is worse.

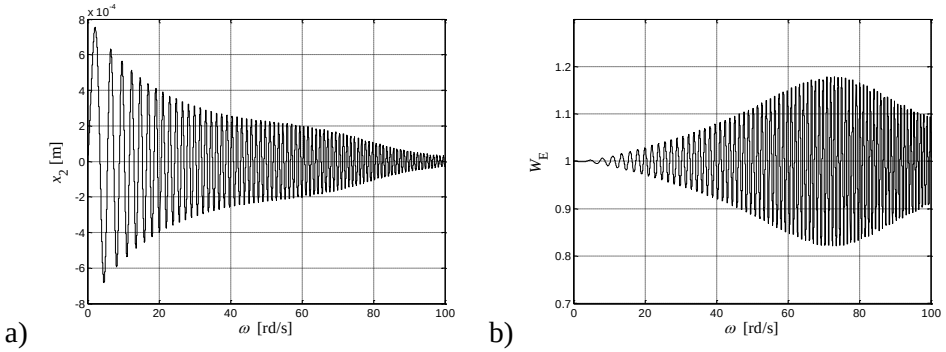

a) b)

Fig. 3. LQR controller (α_x=100, α_v=1, ρ=0.1, σ=100 [1/s]): a) displacement x_2, b) Eusam index W_E

For the values α_x=100 and ρ=0.1 in the wide frequency range, both the amplitude of vibration (Fig. 3a) and the Eusam index (Fig. 3b) are satisfactory. E.g. within the range of the first resonance an reduction in displacement amplitude by eight times is visible (x_{2max}<0.6mm for ω≈8.4rd/s and a=5mm), while in the range of second resonance, index W_E >0.8.

In order to better illustrate the effect of control parameters on the selected frequency characteristics, in the following figures (Fig. 4, 5, 6) the maximal (or minimal in case of the Eusam index) values of response of the system to excitation defines by Eqs (22-24), are shown.

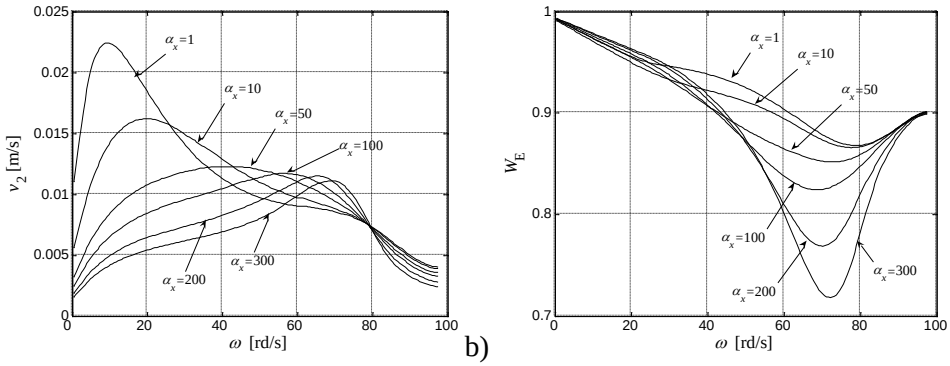

a) b)

Fig. 4. LQR controller – effect of parameter α_x (α_v=1, ρ=0.1 and σ=100 [1/s]), a) velocity v_2, b) Eusam index W_E

Fig. 4 shows the velocities (Fig. 4a) and Eusam index (Fig. 4b) as functions of excitation frequency, acquires for the system with LQR for six different values of parameter α_x and α_v=1, ρ=0.1, σ=100 1/s. With the increase of parameter α_x the

decrease in displacement, velocities and accelerations in the low-frequency range is notable, but the Eusam index (as well as the momentary power) is increased near the second resonance.

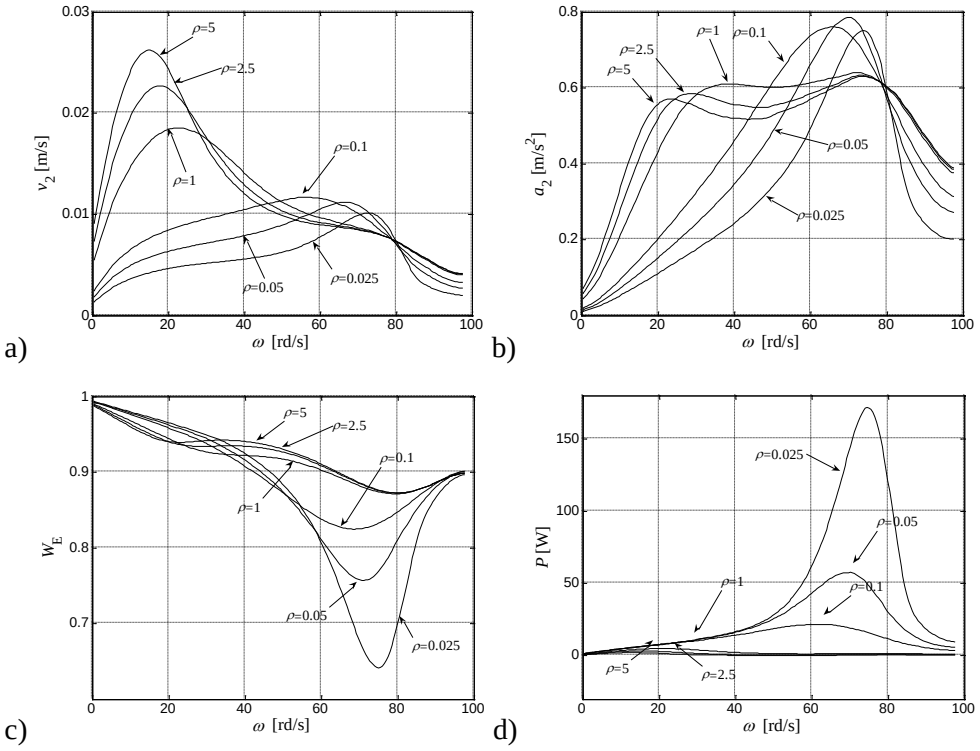

Fig. 5. LQR controller– effect of parameter ρ (α_x=100, α_v=1, σ=100 [1/s]):
a) velocity v_2, b) acceleration a_2, c) Eusam index W_E, d) momentary power P

Fig. 5 shows the effect of parameter ρ on the frequency characteristics of the system. When the value ρ decreases, both the velocities and displacements decrease as well (Fig. 5a), while the acceleration of the spring-supported mass are relatively low within the low-frequency range (Fig. 5b). As the lower values of parameter ρ require less restrictions imposed on the control signal, with the decrease of its value, the control forces, Eusam index (Fig. 5c) and the momentary power (Fig. 5d) begin to rise (rapidly at ρ<0.05)

The effect of time delay between the control signal u – force U, (Fig. 6 – velocities and power), is notable within the high-frequency range. In a relatively wide range, with the increase of parameter σ (larger time delay), both the vibration of the spring-supported mass (Fig.6a), ale the value of dynamic reaction increase, which causes the minimal value of Eusam index to decrease. Within this range high values of power (Fig. 6b), denoting the changes in energy introduced to the

system, can be see. Although the parameters of control are chosen to be optimal, the active system is not very effective in this range of frequencies.

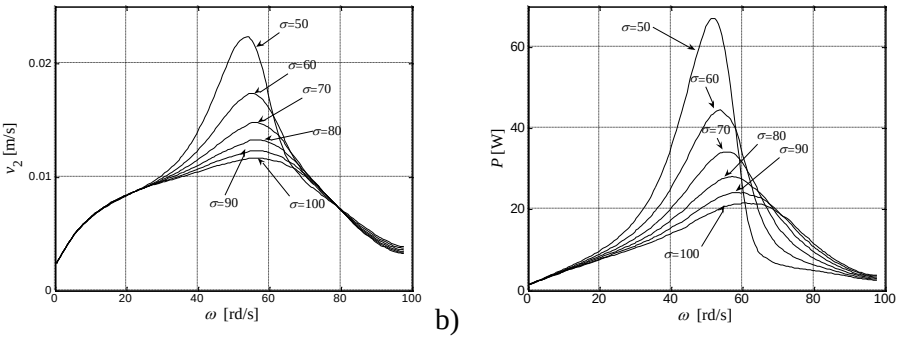

Fig. 6. LQR regulator – effect of parameter σ (α_x=100, α_v=1, ρ=0.1): a) velocity v_2, b) momentary power

Fig. 7 shows the displacements and Eusam index for the SMC regulator, obtained in the similar way as for LQR (Fig. 3). The numerical simulations are performed for β_x=β_v=1, γ=0.1 and σ=100 1/s. Function sgn(S), present in Eq. (17), is approximated by a continuous function $2/\pi$·arctg(ηS), with the parameter η=100. In case of SMC regulator, much better vibration reduction can be accomplished (Fig. 7a) than for LQR (Fig. 3a), especially in the low-frequency range. Similar, as with LQR, within the high-frequency range both the Eusam index (Fig. 7b), and the momentary power (not shown here), are unsatisfactory.

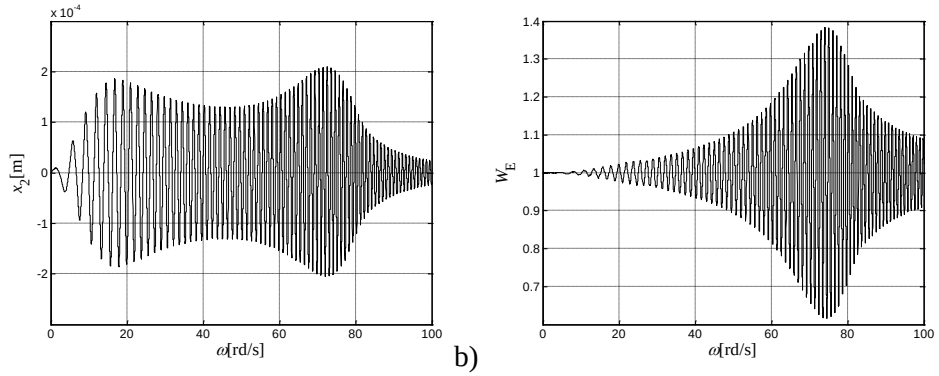

Fig. 7. SMC regulation (β_x=β_v=1, γ=0.1, σ=100 [1/s]): a) displacement x_2, b) Eusam index W_E

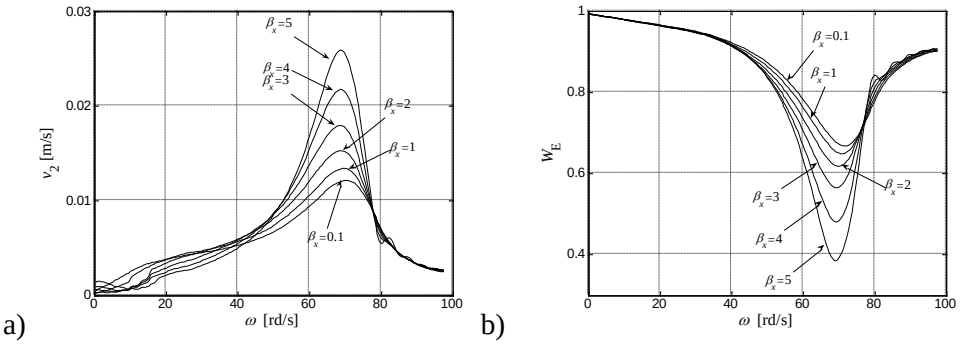

Fig. 8. SMC regulation – effect of parameter β_x (β_v=1, γ=0.1, σ=100 [1/s]):
a) velocity v_2, b) Eusam index W_E

Fig. 8 shows the characteristics of SMC regulator obtained for six different values of parameter β_x. The effect of parameter β_x on the frequency characteristics, is apart from the slightly different plot, similar to the parameter α_x for LQR (Fig. 4). With the increase in β_x the amplitude of vibration decreases in the lower frequency range. However, if this value is too high, the so-called effect of „chattering" might occur, which causes the characteristic of the system to greatly inferior in the high-frequency range.

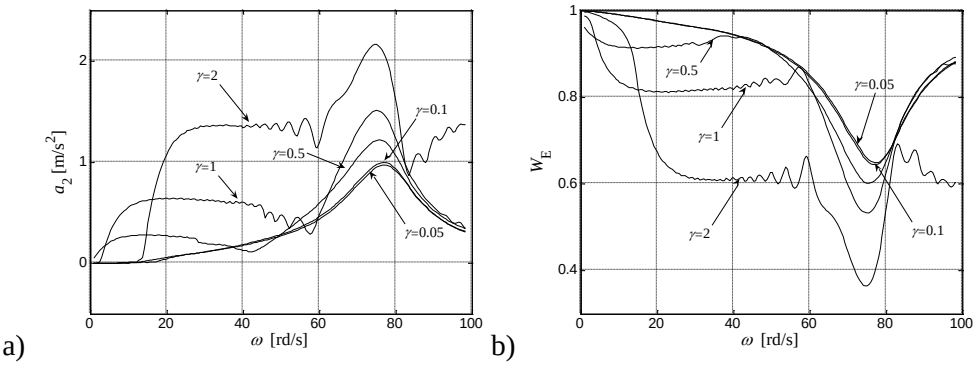

Fig. 9. SMC regulation – effect of parameter γ (β_x=β_v=1, σ=100[1/s]):
a) acceleration a_2, b) Eusam index W_E

The „chattering" effect – the appearance of high frequency oscillation, is caused mostly by the switching component of control $u^{sw}(t)$, visible in the time plots. This effect is also the cause for the irregular frequency characteristics plots. Fig. 9a (maximal accelerations) and Fig. 9b (Eusam index), obtained for β_x=β_v=1, σ=100[1/s] and five different values of γ partially illustrate the effect of

„chattering". From the analysis of numerous results of numerical simulations, a conclusion can posed, that with the increase of parameter γ (and also β_x) the vibration amplitudes decrease in the range of first resonance, but for the excitation of high frequency, the maximal value of control force is increased, while the minimal value of Eusam index is decreased (Fig. 9b). Additionally, after exceeding certain values (for γ>0.1) the rapid rise in accelerations in noticeable (Fig. 9a) and the possibly of "chattering" effect occurring is high.

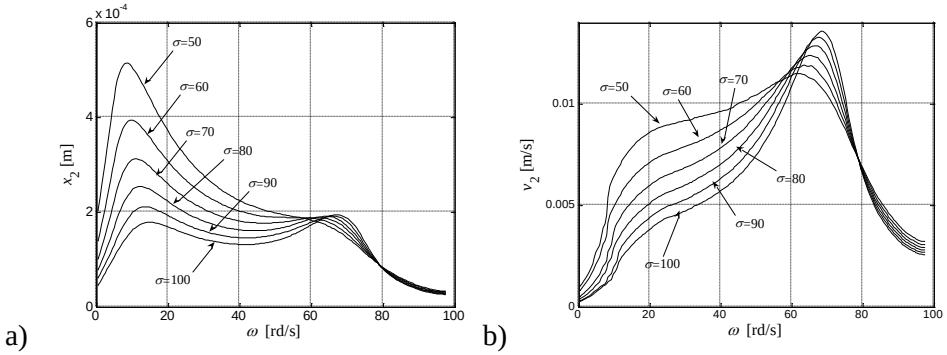

a) b)

Fig. 10. SMC regulation – effect of parameter σ (β_x=β_v=1, γ=0.1): a) velocity v_2, b) momentary power

The frequency characteristics of the system depend also on the value of parameter σ. This influence is visible in Fig. 10, obtained for six value of σ and β_x=β_v=1, γ=0.1. With the increase of σ the regulator is more effective in the low-frequency range (Fig. 10a – velocities, 10b - accelerations), however its efficiency is greatly decreased in the second resonance range, and the power requirement is much higher, especially for high values of parameter β_x (for β_x>1).

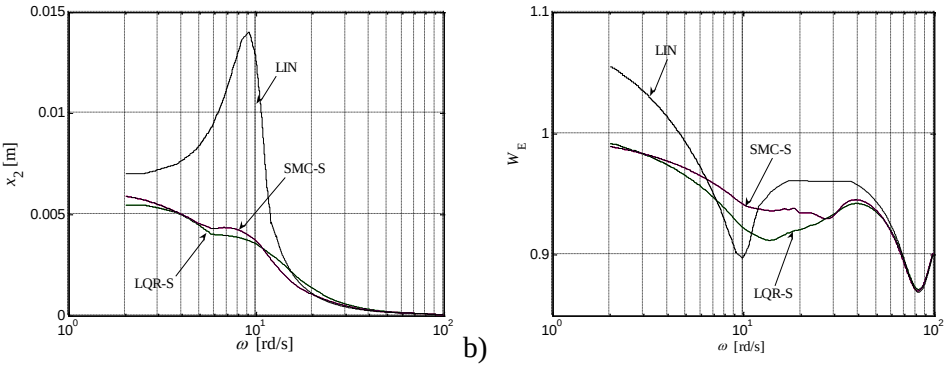

a) b)

Fig. 11. Comparison of semi-active LQR-S, SMC-S and passive LIN system (σ=100 rd/s): a) displacement x_2, b) Eusam index

Fig. 11 shows the frequency characteristics of semi-active LQR (denoted as LQR-S) for $\alpha_x=\alpha_v=1$ and $\rho=0.1$ and also SMC (SMC-S) for $\beta_x=\beta_v=1$ anf $\gamma=0.1$. Additionally a characteristic of a system without regulator is presented (LIN).

For the parameters chosen as such, the efficiency of the semi-active damper is satisfactory both in terms of driving comfort (Fig. 11a) and safety (Fig. 11b) Within the range of first resonance, both semi-active system are thrice as effective as the passive system, in the high-frequency range on the other hand, the performance of semi-active and passive systems is compatible. Semi-active regulators, when compared to the active ones, are less vulnerable to the changes of parameter σ. In the calculations, these values were assumed: $\sigma=100$ 1/s and $u_{\max}=10K_u$.

It need to be pointed out, that the value of parameter α_x for LQR-S is different from the one used for the LQR. For the previously used values of parameters α_x, α_v and ρ the system with LQR-S controller, does not behave well in the low-frequency regime (below to 60 rad/s). The SMC-S regulator, works well when the parameters β_x and γ are low, but the effect of parameter β_x is less significant than in the case of active control – that is why, the same value as for the SMC, is used in the calculations.

Both semi-active systems, reduce the amplitude of displacement to a same degree, and although these are both less effective in the minimization of vibration when compared to the active systems, when compared in terms of driving safety both are better, due to the much higher minimal values of Eusam index.

The similar operation of LQR-S and SMC-S, is most probably the effect of similar force characteristics generated by both regulators. Fig. 12 and 13 show the relation between the control force and the relative velocity for LQR-S ($\alpha_x=\alpha_v=1$, $\rho=0.1$) and SMC-S $\beta_x=\beta_v=1$, $\gamma=0.1$) systems.

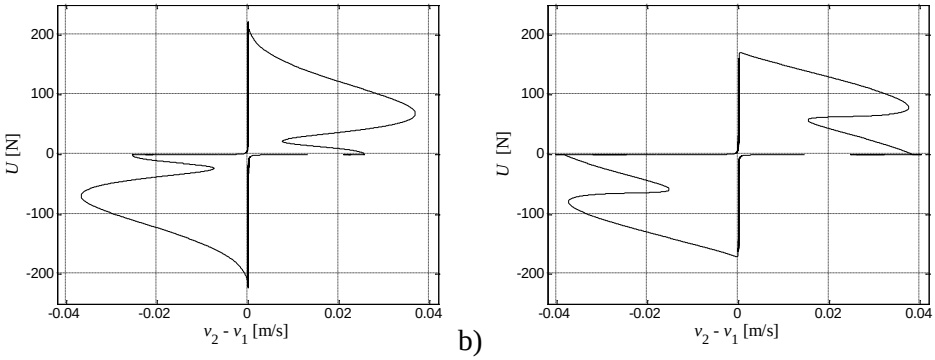

Fig. 12. Control force characteristic (ω=8.396 rd/s and a=5mm, σ=100 rd/s): a) LQR-S, b) SMC-S

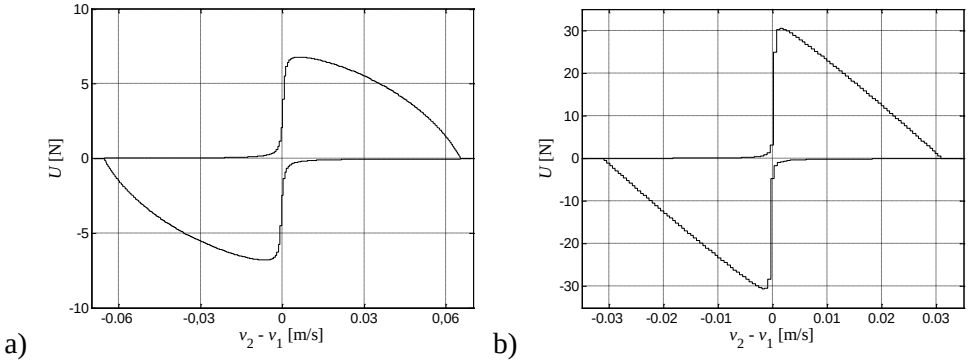

a) b)

Fig. 13. Control force characteristic (ω=84.39 rd/s, a=0.4mm, σ=100 rd/s): a) LQR-S, b) SMC-S

It was assumed, that the system is exposed to harmonic excitation defined by the parameters: ω=8.396 rd/s and a=0.005m (first resonance) and ω=84.39 rd/s and a=0.0004m (second resonance). The plot of the characteristics in the first and third quadrant of the system is due to the condition imposed on the momentary power. Less-than-ideal plot of the curve in those quadrants is the result of replacing a discontinuous function (20) by a continuous one. For the angular frequency ω=8.396 rad/s both characteristics are similar, both in quality and quantity sens. For the second resonance, the differences are more significant, with the visibly higher control force values of SMC-S.

7. Conclusions

From the analysis of the results and observations, obtained for numerical simulation performed under different conditions, several conclusions can be posed:

- The application of both active systems, especially the SMC algorithm, greatly reduces the values amplitude, velocity and acceleration within the frequency range close to first resonance value, which in turn slightly increases the comfort of passenger during the drive.
- Active systems are however unsatisfactory, within the range of second resonance frequency, as they cause the Eusam index to decrease, which defines how well the wheel-road adhesion is, and also increase the momentary power, and so the energy that needs to be introduced to the system
- The analyzed systems, especially the active controllers, are sensible to time delay between the regulator and the actuator. This fact should be taken into consideration when choosing the parameters of the regulator

- The semi-active systems are visibly less effective within the region of first resonance frequency, however due to their lower cost and higher resistance to control signal time delays, they can become an alternative to the active systems.

References

[1] Ahmadian M., Vahdati N., 2006, Transient dynamics of semiactive suspensions with hybrid control, *Journal of Intelligent Material Systems and Structures*, **17**, 2, 145-153

[2] Chen P.-C., Huang A.-C., 2005, Adaptive sliding control of non-autonomous active suspension systems with time-varying loadings, *Journal of Sound and Vibration*, **282**, 1119-1135

[3] Fischer D., Isermann R., 2004, Mechatronic semi-active and active vehicle suspensions, *Control Engineering Practice*, **12**, 1353-1367

[4] Gopala Rao L.V.V., Narayanan S., 2009, Sky-hook control of nonlinear quarter car model traversing rough road matching performance of LQR control, *Journal of Sound and Vibration*, **323**, 515-529

[5] Huang S-J, Chen H-Y., 2006, Adaptive sliding controller with self-tuning fuzzy compensation for vehicle suspension control, *Mechatronics*, **16**, 607-622.

[6] Lin J., Lian R-J, Huang C-N, Sie W-T., 2009, Enhanced fuzzy sliding mode controller for active suspension systems, *Mechatronics*, **19**, 1178-1190

[7] Liu Y., Waters T.P., Brennan M.J., 2005, A comparison of semi-active damping control strategies for vibration isolation of harmonic disturbances, *Journal of Sound and Vibration*, **280**, 21-39

[8] Łuczko J., 2011, Comparison of dynamical responses of semi-active dampers described by the Bouc-Wen and Spencer models (in Polish), *Czasopismo Techniczne*, **2**, 1-M 127-136

[9] Łuczko J., Ferdek U., 2012, Comparison of different control strategy in semi-active vehicle suspension system (in Polish), *Czasopismo Techniczne*, **11**, 6-M, 81-92

[10] Maciejewski I., 2012, Control system design of active seat suspensions, Journal of Sound and Vibration, **331**, 1291–1309

[11] Makowski M., Knap L., Grzesikiewicz W., 2011, Modelowanie i identyfikacja parametrów sterowanych tłumików magnetoreologicznych, *Modelowanie Inżynierskie*, **41**, 261-269

[12] Orman M., Snamina J., 2009, Comparison of effectiveness of semi-active and active cable vibration dampers (in Polish), *Czasopismo Techniczne*, **12**, 3-M, 71-83

[13] Rajeswari K., Lakshmi P., 2008, GA tuned distance based fuzzy sliding mode controller for vehicle suspension systems, *International Journal of Engineering and Technology*, **5**, 1, 36-47

[14] Sam Y.M., Osman J.H.S., 2005, Modeling and control of the active suspension system using proportional integral sliding mode approach, *Asian Journal of Control*, **7**, 2, 91-98

[15] Sam Y.M., Suaib N.M., Osman J.H.S., 2008, Hydraulically Actuated Active Suspension System with Proportional Integral Sliding Mode Control, *WSEAS Transactions on Systems and Control*, **9**, 3, 859-868

[16] Sapiński B., Rosół M., 2008, Autonomous control system for a 3 DOF pitch-plane suspension model with MR shock absorbers, *Computers and Structures*, **86**, 379-385

[17] Snamina J., Kowal J., Wzorek T., 2011, Analysis of the energy dissipation in vehicle suspensions for selected control algorithm (in Polish), *Czasopismo Techniczne*, **2**, 1-M, 233-240

[18] Tomera M., 2010, Nonlinear controller design of a ship autopilot, *International Journal of Applied Mathematics and Computer Science*, **20**(2), 271-280

[19] Wu X., Griffin M. J., 1997, A semi-active control policy to reduce the occurrence and severity of end-stop impacts in a suspension seat with an electrorheological fluid damper, *Journal of Sound and Vibration*, **203**, 5, 781-793

[20] Yildirim S., 2004, Vibration control of suspension systems using a proposed neural network, *Journal of Sound and Vibration*, **277**, 1059-1069

[21] Yoshimura T., Kume A., Kurimoto M., Hino J., 2001, Construction of an active suspension system of a quarter car model using the concept of sliding mode control, *Journal of Sound and Vibration*, **239**, 2, 187-199